Proceedings of the
2007 IEEE Intelligent Vehicles Symposium
Istanbul, Turkey, June 13-15, 2007

Vertical Dynamics Emulation Using a Vehicle Equipped with Active Suspension

Mehmet Akar, Jens C. Kalkkuhl and Avshalom Suissa

Abstract— **This paper presents an integrated active suspension controller for vertical dynamics emulation. The proposed controller consists of an active body controller and a force controller, that are both designed based on mathematical models derived from physical principles and also validated by experimental data. The efficacy of the proposed method is verified by not only realistic simulations in an advanced simulator but also by experiments on a test vehicle.**

Index Terms— **Active suspension control, vehicle emulation, vertical dynamics control**

I. Introduction

Being able to emulate the driving behavior of a range of vehicles using a prototype is useful in the development of advanced passenger cars equipped with computer controlled systems such as 4W steering, active suspension, and cruise control. The vehicle emulation problem that is of interest in this paper is the design of an integrated chassis controller consisting of 4W steering and an active suspension controller in order to track some reference signals corresponding to the vehicle being emulated. To this end, we have developed algorithms to be used for the four wheel steering system to control the vehicle lateral dynamics despite uncertainties in vehicle parameters and external wind disturbances [2], [3]. This paper is focussed on active suspension modelling and control, and it complements our previous work [2], [3] by discussing the details of the vertical controller architecture and emulation capabilities of the test vehicle.

Automobile suspensions are designed for enhanced ride comfort and handling. Conventional passive suspensions achieve these conflicting purposes through the use of springs and dampers. In an active suspension system that is the topic of this paper, the required forces are generated through active elements such as hydraulic pumps. In [4], Yamashita consider a quarter model of a hydraulic active suspension system and design a controller that is based on H^∞ techniques. Tuan et. al. extend the work of [4] by incorporating the semiactive valve as an additional control variable, and by utilizing extensions of nonlinear H^∞ theory [6]. In [5], Smith and Wang derive a parameterization of all stabilizing controllers for disturbance response decoupling and apply their results to vehicle active suspension control assuming a second order actuator model for the active component. A survey of earlier results on active suspension systems with an emphasis on optimal control theory can be found in [7]. Further work on active suspension system modelling and control was reported in [8], [9].

The main contribution of the present paper is an integrated active suspension controller for vertical dynamics emulation. The proposed controller consists of an active body controller and a force controller, that are both designed based on mathematical models derived from the physics of the system and also validated by experimental data. The active body controller design draws heavily upon classical PID techniques and it generates reference forces corresponding to desired lift/pitch/roll/warp motion, whereas the force controller utilizes sliding mode based techniques [10], and it computes the electronic currents required to track these reference forces. The efficacy of the integrated controller is verified by not only realistic simulations in an advanced simulator but also by experiments on a test vehicle.

II. Vertical Dynamics Emulation

Broadly, we are interested in a prototype test vehicle that can emulate the reference vehicle motion in the lateral and vertical directions. To this end, we have developed algorithms to be used for the four wheel steering system to control the vehicle lateral dynamics [2], [3]. The specific objective of this paper is to enable the compact size test vehicle to emulate the vertical dynamics of a range of reference vehicles. Given

This work was partially funded by the EU Project CEmACS 004175.

M. Akar was with the Hamilton Institute, National University of Ireland, Maynooth. He is currently with the Department of Electrical and Electronics Engineering, Boğaziçi University, Bebek, İstanbul {mehmet.akar@nuim.ie, mehmet_akar@yahoo.com}. J. Kalkkuhl and A. Suissa are with DaimlerChrysler, Sindelfingen, Germany.

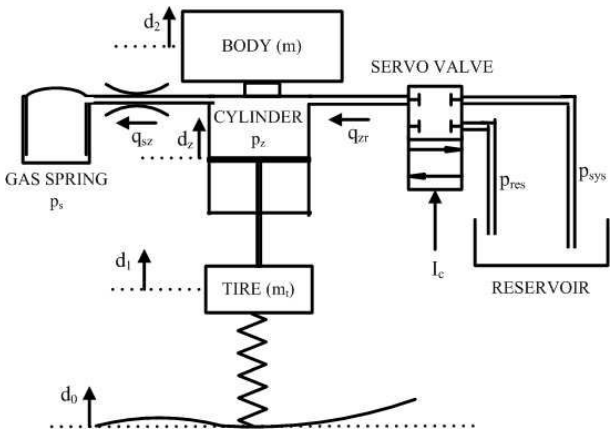

Fig. 1. AHP diagram for a quarter car

m	Quarter–car weight
C_l	Leaf valve flow conductance
A_z	Cross sectional area of the piston
κ	Adiabatic exponent of the gas
k_v	Valve gain
E	Compression module of oil
V_{z0}	Volume of oil at operating point
p_{sys}, p_{res}	Pressure of system and reservoir
p_z, p_s	Pressure of cylinder and gas spring
q_{sz}	Flow from cylinder into gas spring
q_{zr}	Flow from reservoir into cylinder
w_a	natural frequency of valve
η_a	damping coefficient of valve
d_0, d_1, d_2, d_z	Road, wheel, body and cylinder displacement
I_c	Input current to servo valve

TABLE I
NOMENCLATURE

a driver command that produces desired trajectories for lift/roll/pitch for the reference vehicle, i.e., ξ_{ref}, our task is to generate the input currents for the active hydropneumatic (AHP) system on each tire for the test vehicle so that its vertical dynamics mimic those of the reference vehicle despite the possible effect of road disturbances.

A. Transformation into lift/roll/pitch variables

The displacement sensors placed on each suspension system are used to record the relative motion in the vertical direction. By taking into account their geometrical positions on the vehicle, it is convenient to represent the measurements of relative displacements on each tire in terms of lift/roll/pitch variables, i.e.,

$$x = T_A \xi, \ \xi = T_A^{\dagger} x, \tag{1}$$

where x is the 4-dimensional vector of displacements; ξ is the 3-dimensional vector of lift/roll/pitch variables; and $T_A^{\dagger}$ is the pseudo-inverse of T_A [8].

The vehicle emulation problem is to make the vehicle variable ξ track the given reference ξ_{ref}. This requires a good understanding of the AHP suspension system, that is discussed next.

III. AHP Modelling and Validation

We start with a quarter–car model description of the hydro–pneumatic active suspension that is commissioned on the test vehicle. As shown in Fig. 1, the quarter car mass (m) is assumed to sit on a cylinder whose interior pressure is denoted by p_z. The cylinder is connected to a gas spring (with pressure p_s) through a laminar resistance with conductance C_l. The oil flow into and out of the cylinder is controlled through a servo valve by applying an electric current I_c. If the control input I_c is positive, then oil is pumped into the cylinder while a negative current results in a flow of oil from cylinder into the reservoir. The oil flow through the servo valve can be accurately modelled by

$$q_{zr,i} = \begin{cases} k_v \text{sat}(I_c)\sqrt{p_{sys} - p_z} & \text{if } I_c \geq 0, \\ k_v \text{sat}(I_c)\sqrt{p_z - p_{res}} & \text{if } I_c < 0, \end{cases} \tag{2}$$

where p_{sys} is the system pressure that is considerably greater than the cylinder pressure; p_{res} is the reservoir pressure that is close to one bar in normal operating conditions; $\text{sat}(I_c)$ is the saturation function

$$\text{sat}(I_c) = \begin{cases} I_c & \text{if } |I_c| \leq 1, \\ \text{sgn}(I_c) & \text{if } I_c > 1, \end{cases} \tag{3}$$

and $\text{sgn}(I_c)$ is the signum function

$$\text{sgn}(I_c) = \begin{cases} 1 & \text{if } I_c > 0, \\ -1 & \text{if } I_c < 0. \end{cases} \tag{4}$$

The oil flow in and out of the cylinder is then described by

$$\ddot{q}_{zr} = -w_a^2 q_{zr} - 2\eta_a w_a \dot{q}_{zr} + w_a^2 q_{zr,i}. \tag{5}$$

The flow between the cylinder and the gas spring can be modelled as a resistor [4]

$$q_{sz} = C_l(p_z - p_s), \tag{6}$$

where C_l is the flow conductance of the leaf valve.

Under the assumption that no heat exchange takes place in the environment, the product $p_s V_s^{\kappa}$ stays constant, i.e.,

$$p_s V_s^{\kappa} = p_{s0} V_{s0}^{\kappa}, \tag{7}$$

where κ is the adiabatic exponent of the gas, and (p_{s0}, V_{s0}) is some initial pressure and volume pair [9]. We also note that the volume change in the gas spring is equal to negative of the flow q_{sz}, i.e.,

$$\dot{V}_s = -q_{sz} = -C_l(p_z - p_s). \tag{8}$$

From (7) and (8), the change in the gas spring pressure is described by the state equation

$$\dot{p}_s = \frac{\kappa C_l}{p_{s0}^{1/\kappa} V_{s0}} p_s^{1+1/\kappa}(p_z - p_s) \tag{9}$$

The pressure change in the cylinder, p_z, is proportional to the volume change with the proportionality constant E/V_{z0}. The change in volume, in turn, is affected from the relative movement of the piston, $\dot{d}_z$, and the flow difference $q_{zr} - q_{sz}$; hence the pressure change in the cylinder is modelled by

$$\dot{p}_z = \frac{E}{V_{z0}} A_z \dot{d}_z - \frac{E}{V_{z0}} C_l (p_z - p_s) + \frac{E}{V_{z0}} q_{zr}. \tag{10}$$

The motion equations for the tire (d_1) and the body (d_2) can be written explicitly [8], [9]. Instead of d_1 and d_2, we will use the plunger displacement variable d_z as our main state variable to characterize the displacement in the vertical direction. There are two main reasons in adapting this reduced order model: The first is to do with the fact that we can measure d_z. Moreover, as shown in [8], [9], a more complicated model would require many more displacement variables with parameters difficult to identify, and no guarantee of better performance. Therefore we propose to use the second order characterization of d_z

$$m\ddot{d}_z = -a_{21} d_z - a_{22} \dot{d}_z - F_c \text{sign}(\dot{d}_z) - d_v \dot{d}_z + a_{23} A_z p_z \tag{11}$$

where $F_c \text{sign}(\dot{d}_z) + d_v \dot{d}_z$ is the friction term, and $A_z p_z$ is the force acting on the plunger.

Hence our reduced order model is

$$\begin{aligned} \ddot{d}_z &= -\tfrac{a_{21}}{m} d_z - \tfrac{a_{22}+d_v}{m} \dot{d}_z - \tfrac{F_c}{m} \text{sign}(\dot{d}_z) + \tfrac{a_{23}}{m} A_z p_z \\ \dot{p}_z &= \tfrac{E}{V_{z0}} A_z \dot{d}_z - \tfrac{E}{V_{z0}} C_l (p_z - p_s) + \tfrac{E}{V_{z0}} q_{zr} \\ \dot{p}_s &= \tfrac{\kappa C_l}{P_a^{1/\kappa} V_a} p_s^{1+1/\kappa} (p_z - p_s) \end{aligned} \tag{12}$$

with q_{zr} from (2) and (5). The above model has been validated with the real data from the test vehicle. The results are shown in Figs. 2–3. In particular, it is noted from Fig 2 that the prediction error in the cylinder pressure is less than five percent, whereas the displacement of the plunger can be modelled quite accurately as seen in Fig 3.

IV. Controller Design

The controller architecture implemented on each tire is shown in Fig. 4, where d_r is the road disturbance and y_m is the measurement vector of pressures and displacements. The proposed controller loop consists of two sub-controller blocks: The Active Body Controller (ABC) and the Force Controller (FC). Given

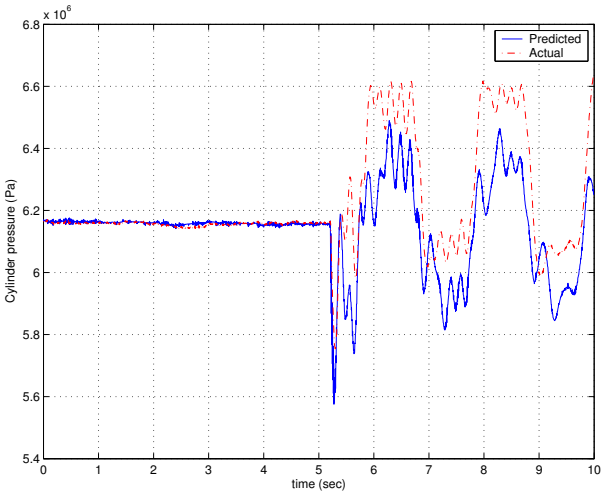

Fig. 2. Predicted and actual cylinder pressures (right rear tire).

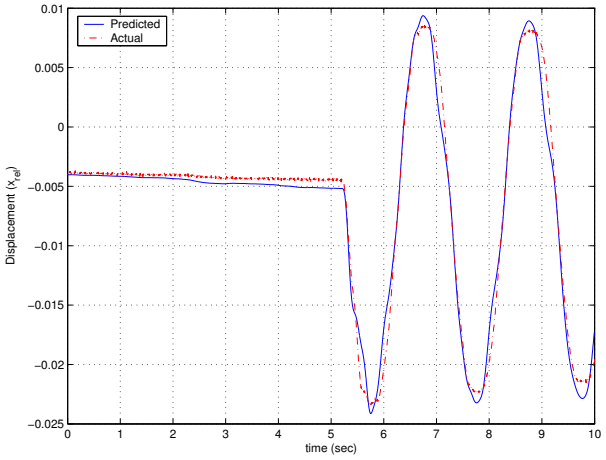

Fig. 3. Actual and predicted plunger displacements (in meters).

desired vertical dynamics ξ_{ref} and measurements, the ABC generates a desired force F_{ref} which is then fed into the force controller to determine the input current I_c to be applied to the AHP system. In the sequel, we discuss both the ABC and the FC in detail.

A. Active Body Controller (ABC)

The objective of the active body controller is to generate the *desired* force, $F_{ref} \in \Re^4$, in order to induce some desired displacement on each suspension system. Given the reference signal $\xi_{ref} \in \Re^3$, the task is to design an outer control loop that will track the desired lift/roll/pitch dynamics. Let

$$e_\xi = \xi_{ref} - \xi, \tag{13}$$

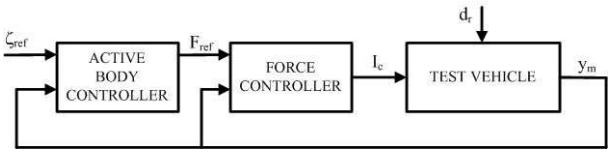

Fig. 4. Vertical controller architecture.

be the tracking error. The controller is a linear controller with the diagonal matrix transfer function

$$C_\xi(s) = \text{diag}\{C_{lift}(s), C_{roll}(s), C_{pitch}(s)\}, \quad (14)$$

where $C_{lift}(s)$, $C_{roll}(s)$, and $C_{pitch}(s)$ are PID type controllers, whose proportionality constants are to be chosen appropriately. The output of the controller $\mathcal{L}^{-1}(C_\xi(s)E_\xi(s))$ is a 3-dimensional vector which is then transformed into the references forces

$$F_{ref}(t) = T_R\mathcal{L}^{-1}(C_\xi(s)E_\xi(s)), \quad (15)$$

where T_R is a 4×3 transformation matrix.

1) Choice of the Controller Parameters: The choice of the controller parameters for the ABC relies on the linearized version of the validated model we have obtained in the previous section. In particular, the plant is given by

$$G(s) = \text{diag}\{G_z(s), G_z(s), G_z(s), G_z(s)\}, \quad (16)$$

where

$$G_z(s) = \frac{\bar{b}}{s^2+\bar{a}_1 s+\bar{a}_2}, \quad (17)$$

$$\bar{b} = a_{23}/m,\ \bar{a}_1 = (a_{22}+d_v)/m,\ \bar{a}_2 = a_{21}/m \quad (18)$$

The controller parameters are chosen such that the closed loop transfer function

$$\left(I + G(s)T_R C_\xi(s) T_A^\dagger\right)^{-1} G(s)T_R C_\xi(s), \quad (19)$$

is stable, and the plunger acceleration errors in the human sensitivity range (3-8 Hz) are attenuated. In the implementation of the controller on the test vehicle, several filters have to be used to compensate for noise and measurement offsets. Although not shown here, it is verified that the closed loop system is stable with these additional filters in the loop.

B. Lateral Acceleration Compensation

The reference force in (15) does not take into account the coupling from the lateral dynamics that produce lateral acceleration, which in turn effects the roll dynamics. It is important to cancel this coupling for faster tracking response. Therefore, we modify the reference force in (15) as

$$F_{ref}(t) = T_R\mathcal{L}^{-1}(C_\xi(s)E_\xi(s)) - mha_y[\alpha, -\alpha, 1-\alpha, -1+\alpha]^T, \quad (20)$$

where a_y is the measured lateral acceleration, h is the center of gravity height, and α is a parameter in the interval $(0, 1)$ ($\alpha = 0.5$ in implementation).

C. Force Controller (FC)

Given a reference force F_{ref} that translates into a reference cylinder pressure $p_{z,ref=F_{ref}/A_z}$, the objective of the force controller is to make the cylinder pressure p_z track the reference value $p_{z,ref}$. With a slight abuse of notation, in the sequel we will be discussing one dimensional variables corresponding to individual tires. Let

$$e_{p_z} = p_z - p_{z,ref}, \quad (21)$$

$$\sigma = e_{p_z} + \lambda_1 \int_0^t e_{p_z}(\tau)d\tau. \quad (22)$$

First, the desired flow is computed as

$$q^*_{zr} = -\frac{E}{V_{z0}}A_z\dot{d}_z + \frac{E}{V_{z0}}(p_z - p_s) + \dot{p}_{z,ref} - \lambda_1 e_{p_z} - \lambda_2\sigma - M\text{sgn}(\sigma). \quad (23)$$

where λ_1, λ_2 and M are positive controller design parameters. The electronic current to be applied is determined from

$$I^*_c = \begin{cases} \frac{q^*_{zr}}{k_v\sqrt{p_{sys}-p_z}} & \text{if } q^*_{zr} \geq 0, \\ \frac{q^*_{zr}}{k_v\sqrt{p_z-p_{res}}} & \text{if } q^*_{zr} < 0, \end{cases} \quad (24)$$

The following observations can be made on the FC:

1) It can be shown that the force controller in (24) takes the trajectories to the sliding manifold $\sigma = 0$ in finite time; and both e_{p_z} and $\dot{e}_{p_z}$ converge to zero. The closed loop stability requires the controller parameters λ_1 and λ_2 to be positive, whereas the gain M is chosen high enough in implementation to overcome probable uncertainties in the system description.
2) The linearized version of (9) around the operating point is given by

$$\dot{p}_s = \frac{\kappa C_l}{p_{s0}^{1/\kappa}V_{s0}}p_{ref}^{1+1/\kappa}(p_z - p_s) \quad (25)$$

Since p_z tracking error converges to zero exponentially fast, it follows from the above equation that p_s will converge to p_z as well.

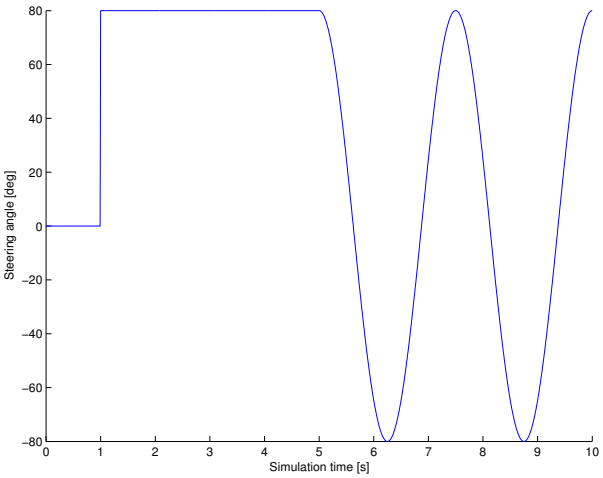

Fig. 5. Driver maneuver.

3) Error dynamics of the FC is given

$$\dot{e}_{p_z} + \lambda_1 e_{p_z} = 0. \tag{26}$$

Hence the responsiveness of the FC can be controlled by suitably choosing λ_1.

4) The FC can be modified by removing either or both of the terms including $\dot{d}_z$, and $p_z - p_s$ in (23), and suitably choosing the controller gain M. The previous comments on the performance of the FC are still valid for its modified versions.

V. Numerical Analysis

A. Simulation Results

We first investigate the emulation capabilities of our controller via simulations in an advanced car simulator provided by DaimlerChrysler. Specifically, we will consider the emulation of three classes of vehicles: Commercial van, S–class, and a bus. Given one of these vehicles to emulate, the simulation results are presented for the driver maneuver depicted in Fig. 5. For the given maneuver that is a step steering of 80 degrees for 4 seconds followed by slalom driving, a desired roll angle is generated for each vehicle to emulate, and the desired pitch/warp/lift values are set to zero.

Fig. 6 summarizes the simulation results for commercial van emulation. As seen in Fig. 6(b), the force tracking is excellent on all suspension systems. The roll tracking is also very good even though such a maneuver creates a lateral acceleration that is well beyond the linear operation of the vehicle.

The emulation results for a bus and an S–class are shown in Figs. 7 and 8, respectively. Once again, the

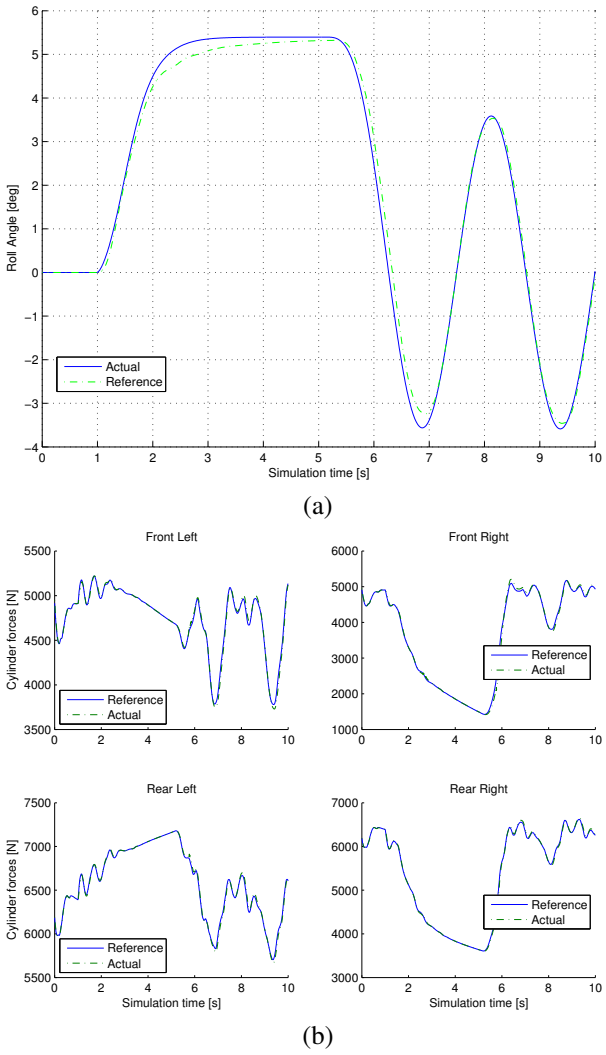

Fig. 6. Commercial van emulation in advanced simulator.

tracking capability of the controller is quite amazing. Hence, from Figs. 6–8, we can conclude that vertical dynamics emulation of a wide range of ground vehicles can be carried using the test vehicle.

B. Experimental Tests

We have also examined the performance of the proposed vertical controller in standstill tests. In the standstill tests to be presented, the reference roll angle is a 1.15 degree amplitude sine wave with 0.5 Hz frequency, while the reference signals for pitch and lift are set to zero. The results are summarized in Figs. 9–10. As seen in Fig. 9, the roll tracking error is decreased asymptotically. Furthermore, the reference force tracking as illustrated in Fig 10 is quite impressive.

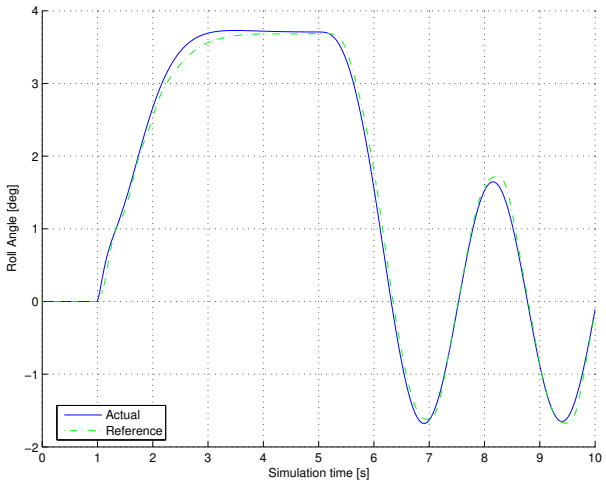

Fig. 7. Bus emulation in advanced simulator.

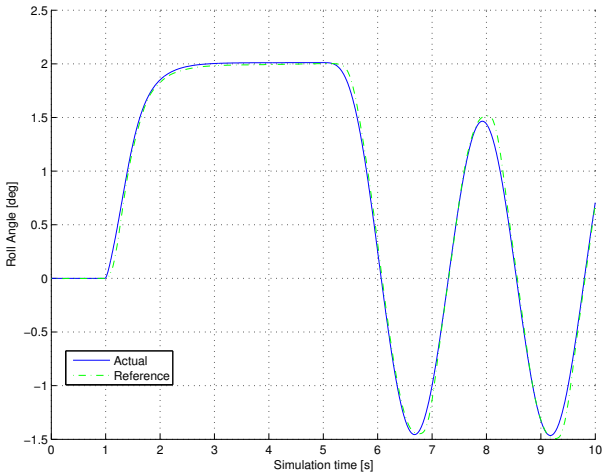

Fig. 8. S–class emulation in advanced simulator.

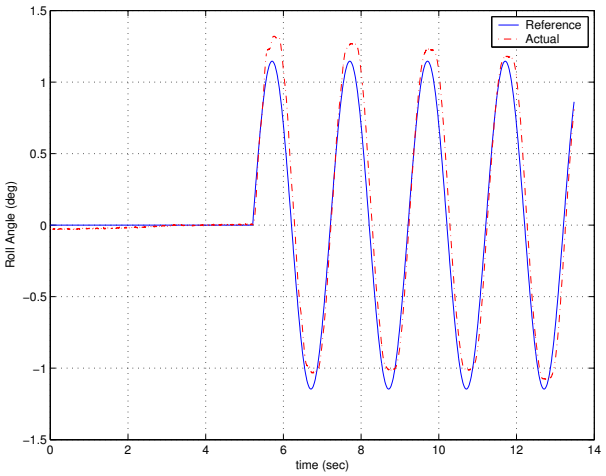

Fig. 9. Experimental results: Roll angle tracking.

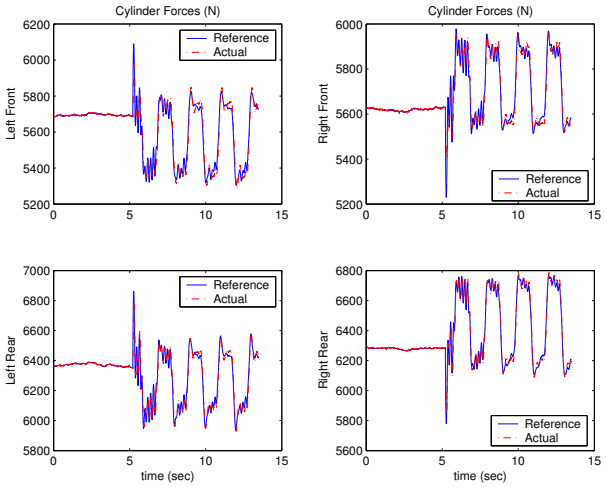

Fig. 10. Experimental results: Cylinder force tracking.

REFERENCES

[1] A. Lee, "Emulating the lateral dynamics of a range of vehicles using a four-wheel-steering vehicle", SAE Paper No. 950304, *International Congress and Exposition*, Detroit, Michigan, USA, 1995.

[2] M. Akar, "Yaw rate and sideslip tracking for 4–wheel steering cars using sliding mode control", *Proceedings of the IEEE International Conference on Control Applications*, Munich, Germany, October 2006.

[3] C. Villegas, M. Akar, R. N. Shorten, and J. Kalkkuhl, "A robust PI controller for emulating lateral dynamics of vehicles", *Proceedings of the 2007 IEEE Intelligent Vehicles Symposium*, Istanbul, Turkey, June 2007.

[4] M. Yamashita, K. Fujimoro, C. Uhlik, R. Kawatani and H. Kimura, "H_∞ control of an automotive active suspension", *Proceedings of the 29th Conference on Decision and Control*, pp. 2244–2250, Honolulu, Hawaii, December 1990.

[5] M. C. Smith and F.-C. Wang, "Controller parametrization for disturbance response decoupling: Application to vehicle active suspension control", *IEEE Transactions on Control Systems Technology*, vol. 10, no. 3, pp. 393–407, May 2002.

[6] H. D. Tuan, E. Ono, P. Apkarian, and S. Hosoe, "Nonlinear H_∞ control for an integrated suspension system via parametrized linear matrix inequality characterizations", *IEEE Transactions on Control Systems Technology*, vol. 9, no. 1, pp. 175–185, January 2001.

[7] D. Hrovat, "Survey of advanced suspension developments and related optimal control applications", *Automatica*, vol. 33, no. 10, pp. 1781–1817, 1997.

[8] E. Duplitzer, *Identifikation und Validierung einers Modells für eing Fahrzeug mit aktivem Fahrwerk*, Studienarbeit, Daimler-Benz, Stuttgart, January 1996.

[9] M. Rau, *Modellierung, Simulation and Auslegung eines hydropneumatischen Federbeins mit schnell verstellbarer Dämpfung*, Diplomarbeit, Universität Stuttgart, 2001.

[10] V. I. Utkin, *Sliding modes in control and optimization*, Springer–Verlag, Berlin, 1992.